

On the Diversity of Non-Linear Transient Dynamics in Several Types of Complex Networks

Luciano da Fontoura Costa

*Institute of Physics at São Carlos, University of São Paulo,
PO Box 369, São Carlos, São Paulo, 13560-970 Brazil*

(Dated: 15th Dec 2007)

Dynamic systems characterized by diversified evolutions are not only more flexible, but also more resilient to attacks, failures and changing conditions. This article addresses the quantification of the diversity of non-linear transient dynamics obtained in undirected and unweighted complex networks as a consequence of self-avoiding random walks. The diversity of walks starting at a specific node i is quantified in terms of a signature composed by the entropies of the node visit probabilities along each of the initial steps. Six theoretical models of complex networks are considered: Erdős-Rényi, Barabási-Albert, Watts-Strogatz, a geographical model, as well as two recently introduced knitted networks formed by paths. The random walk diversity is explored at the level of network categories and of individual nodes. Because the diversity at successive steps of the walks tends to be correlated, principal component analysis is systematically applied in order to identify the more relevant linear combinations of the diversity entropies and to obtain optimal dimensionality reduction. Several interesting results are reported, including the facts that the diversity tends to increase with the average degree for all considered network models and that the Watts and Strogatz and geographical models tend to yield diversity entropies which increase more gradually with the number of steps, contrasting sharply with the steep increases verified for the other four considered models. The principal linear combination of the diversities identified by the principal component analysis method is shown to allow an interesting partitioning of networks into subgraphs of similar diversity.

PACS numbers: 89.75.Fb, 02.10.Ox, 89.75.Da

*‘There is a city where you arrive for the first time; and there is another city which you leave never to return.’
(Invisible Cities, I. Calvino)*

I. INTRODUCTION

The diversity of dynamics plays a key role in most aspects of nature, which has ultimately resulted in a wealthy of species along evolution as well as a myriad of human cultural manifestations. Because of their capacity to represent discrete structures and scaffold dynamics, complex networks (e.g. [1, 2, 3, 4, 5]) have become the key paradigm in theoretical and applied studies in complex dynamic systems, finding applications in an impressive range of problems (e.g. [5]). A great deal of the current attention in this area concentrates not only in characterizing the topological properties of networks (e.g. [5]), but also in investigating how the latter constrains or even define dynamics unfolding in the networks (e.g. [3, 4]).

With a tradition extending back over several decades, the study of the dynamics of random walks represents one of the main paradigms in statistical physics and dynamical systems. Traditional random walks are usually performed by one or more agents choosing with uniform probability between the outgoing edges at each node. Therefore, random walks represent one of the least intelligent ways to move in a network, involving no additional criterion rather than uniform chance. Still, such a dynamics is directly related to the important linear dynamics of diffusion (e.g. [6, 7]), which plays an important

role in a large number of natural dynamical processes (e.g. reaction-diffusion and Schrödinger equation). The dynamics of traditional, linear, random walks on complex networks has been investigated by several articles (e.g. [8, 9, 10, 11, 12, 13]). Several other types of random walks have also been considered in the literature (e.g. [14, 15, 16]). For instance, the category of *self-avoiding* random walks represents a particularly interesting situation in which the moving agent is not allowed to return to nodes and/or edges. As such, self-avoiding walks are can be directly associated to the paths existing in the networks. By *path*, it is henceforth meant a sequence of adjacent [24] edges without repetition of node or edge. Paths are important because they provide the most effective way to connect the involved nodes (i.e. given M nodes, a path through them involves $M - 1$ edges). In addition, unlike random walks, random self-avoiding walks — *path-walks* for short — are non-linear and necessarily finite in finite networks, because the moving agent sooner or later has no way to proceed. The possibility to use self-avoiding walks to sample networks has been investigated in [15]. Paths and self-avoiding walks have recently been explored as dual motifs of star connectivity [17], building block of networks [18] and for characterization of networks (especially through the longest path) [19]. The transient dynamics of self-avoiding walks in uniformly random, small world and scale free networks has been studied in [20, 21], with special attention placed on the average number of such walks.

Random walks typically start from a node and proceed [25] until some stopping condition is met (e.g. fixed

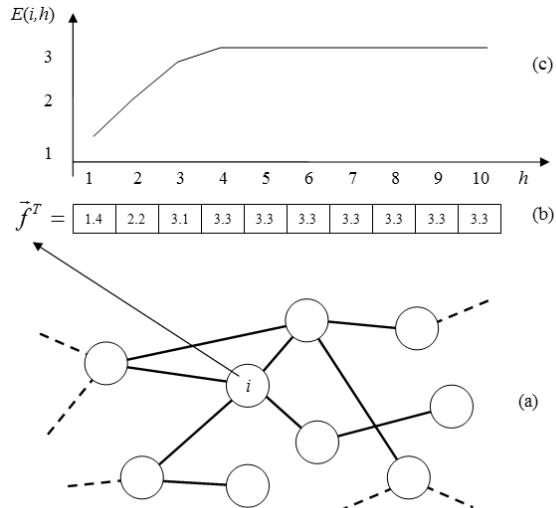


FIG. 1: Given a node i in a network (a), the entropies $E(i, h)$ of the probabilities of visited nodes after the initial h steps (c) can be calculated by simulating several self-avoiding random walks starting from i . Therefore, a signature \vec{f} (b) can be assigned to each node i which expresses the diversity of paths obtained at each step h .

number of steps or, in the case of self-avoiding walks, impossibility to proceed further). In this work all walks are performed for a pre-specified number of 10 steps, as we are interested in the transient dynamics. Consider now that the starting node has been fixed and several self-avoiding random walks are performed from that node. One interesting question regards how such walks are composed and distributed. For instance, one may be interested in the length of these walks (e.g. [19, 20]). A question of special relevance which has received little attention from the literature regards the *diversity* of the obtained walks and path-walks. By diversity, it is meant how much the walks differ one another by incorporating distinct nodes and/or edges. In a previous approach to this problem, Herrero investigated the average number of self-avoiding walks defined in uniformly random and scale free networks. In the present article, the diversity of self-avoiding walks starting at a specific node i is quantified in terms of the entropies of the node probability visits after the first S steps along the walk after starting from each node i , giving rise to diversity entropy (see Figure 1). Because of the non-linear nature of this type of walks and our interest in obtaining information about each individual walk in several types of structurally diverse networks, the visit probabilities are estimated by performing several self-avoiding walks.

Provided such a diversity of dynamics can be quantified, ideally in terms of a single measurement, a series of interesting analyses can be performed at several levels

(e.g. from individual node to network category levels). Indeed, the diversity of walks is immediately related to a large number of important theoretical and practical aspects of complex networks structure and dynamics. To begin with, the cases in which the path-walks are found to be mostly similar (i.e. little diversity) imply that the agent had little choice during its motion, and therefore little path redundancy is present in the network, starting from that node. At the same time, such situations will also be characterized as being highly efficient as far as node coverage is concerned (relatively few edges are required while visiting several nodes). Indeed, by recalling that all nodes in a path-walk must be distinct, a path-walk involving $S + 1$ nodes will necessarily have S edges, which is the minimum number of connections required to connect those nodes. On the contrary, in case the path-walks are found to be strongly diverse, we can conclude that the progression of the agent is characterized by great freedom of choice and variety of transient dynamics. Consequently, because the path-walks can not repeat nodes, we also have that the self-avoiding walks in this case will also involve several diverse nodes. Therefore, nodes with high diversity constitute natural candidates as distributing sources (e.g. for information or mass). It is also important to observe that the dynamics diversity of a node provides information which is complementary to other measurements of network nodes. For instance, though diversity tends to be correlated with the node degree at the initial steps of the self-avoiding walks, such a correlation can be quickly lost as a consequence of the structural diversity at the progressive surroundings of the initial node. The walk diversity is also distinct from the betweenness centrality (e.g. [3, 5]) in the sense that chained nodes with high betweenness centrality will lead to low walk diversity. Therefore, diversity can be best thought as a novel measurement which can complement previous approaches in the characterization of the structural properties of complex networks.

Many are the interesting applications of such diversity studies to real-world problems. For instance, in case the random walks are used to model the acquisition of knowledge or cultural values by the agent (in this case each node represent a knowledge or cultural fact, e.g. [16]), the diversity measurements can provide sound basis for discussing how diverse the development of agents starting from similar backgrounds but subsequently exposed to different information will be. Another particularly interesting application concerns the objective quantification of the diversity of life and species along phylogenetics, as well as geographical exploration. In addition to its potential for the objective characterization of dynamics performed in complex networks, the quantification of the diversity of random walks and path-walks can also provide valuable indications about the structure of the respective networks. For instance, in case all path-walks are identical, we have a chain of nodes extending from the starting node. Contrariwise, a high diversity implies the presence of redundancies in the network.

Because the diversity entropies at subsequent steps tend to be correlated, the statistical method known as *principal component analysis* (PCA) [22] is systematically applied in this work in order to decorrelate those measurements. The PCA method provides an optimal stochastic linear transformation in the sense of concentrating the variation of the data along the first new random variables. In other words, the PCA transforms the original measurements into new features which are completely uncorrelated one another. Because of the linear nature of PCA, the new obtained measurements correspond to linear combinations of the original features, weighted so as to optimize the concentration of variance along the first new variables.

The manuscript starts by presenting the basic concepts, adopted network models, as well as the definition of the diversity entropy and some of its properties. The results are presented with respect to the analysis of whole network categories, individual networks, and individual nodes.

II. BASIC CONCEPTS

This section describes the basic concepts and methods used in this article, including network representation and characterization, the 6 adopted complex network models, the definition and estimation of the diversity entropy signature, as well as the stochastic projections methods applied in order to decorrelate the signatures and achieve dimensionality reduction.

A. Complex Networks Representation and Characterization

A unweighted and undirected complex network, formed by N nodes and E edges, can be fully represented in terms of its *adjacency matrix* K , which is symmetric and has dimension $N \times N$. Each existing edge (i, j) implies $K(i, j) = K(j, i) = 1$, with $K(i, j) = K(j, i) = 0$ indicating absence of that edge. Two edges are said to be *adjacent* whenever they share one of their extremities. A *random walk* corresponds to any sequence of adjacent edges $(i_1, i_2); (i_2, i_3); \dots (i_{p-1}, i_p)$. A walk which does not repeat any edge or node, henceforth called *self-avoiding random walk*, defines a *path* in the network. The *length* of a walk or path is equal to the number of its constituent edges. The shortest path between two nodes is defined as one of the paths between those nodes which has the smallest length.

The *immediate neighbors* of a node i are those nodes which are connected to i through shortest paths of length 1. The *degree* of a node is equal to the number of edges emanating from that node. The node degree averaged within a network is called its *average degree*. *Extremity nodes* are henceforth understood as those with unit

degree. As such, extremity nodes tend to determine the termination of many self-avoiding walks (no way back for the moving agent from that type of nodes). The *clustering coefficient* of a node i is the ratio between the number of undirected edges between the immediate neighbors of i and the maximum possible number of undirected edges among those nodes.

B. Complex Networks Models

Six theoretical models of complex networks are considered in the present work including four traditional models — Erdős-Rényi (ER), Barabási-Albert (BA), Watts-Strogatz (WS) and a geographical model (GG) — as well as two recently introduced knitted types of complex networks [18] — the path-transformed BA model (PA) and path-regular networks (PN). The ER, BA and WS networks are grown in the traditional way (e.g. [1, 2, 3, 4, 5]). The GG networks in this work are obtained by distributing N nodes within a square with uniform probability and connecting all nodes which are closer than a minimal distance d . The PA and PN networks are obtained as explained in [18]: the PA networks (*path-transformed BA networks*) are obtained by star-path transforming all nodes in an original BA network and the PN (*path regular networks*) model is easily obtained by defining paths involving all network nodes in random order and without repetition.

All networks considered in this article have $N \approx 100$ and $m \approx 3$ or $m \approx 5$ (m is the number of spokes in the added nodes in the BA model), with average degree $\langle k \rangle \approx 2m$. The approximations are a consequence of the statistical variability of the models. For the same reason, the number of nodes N can vary slightly for the GG networks. Because the average degrees considered in this work are relatively large (well above the percolation critical value for ER), most of the nodes in each network belong to the largest connected component, which has been considered for all the analyses reported in this article. The total of rewirings used in the WS case was equal to $0.1E$.

C. Diversity Entropy and its Estimation

The *diversity entropy* is the measurement used in this article in order to quantify the diversity of the self-avoiding random walks obtained for each node i at each step h . Let $p(i, j, h)$ be the probability that a node j be visited after h time steps while moving from the starting node i . Once a self-avoiding walk is terminated (i.e. the moving agent can proceed no further), the moving agent is understood to remain at the final node and contribute to the probabilities and diversities for all remaining steps. The diversity entropy of node i can now be defined as:

$$E(i, h) = - \sum_{j=1}^N p(i, j, h) \log(p(i, j, h)) \quad (1)$$

Given the starting node i , $E(i, h)$ can be understood as the diversity entropy *signature* for that node (see Figure fig:features). Each such signature can be transformed into a single value, e.g by taking the arithmetic or geometric average of its values considering all the steps h .

Figure 2 illustrates several particularly relevant situations regarding diversity entropy signatures. Because of the total absence of branches, the chain network in (a) yield a completely null diversity signature. This means total determinism in the sense that all self-avoiding random walks starting from i will be identical. The presence of a branch at step 3 in the structure in (b) implies the increase of the diversity entropy at this specific step. In the network in (c), the branch occurs at the first step, implying diversity entropy $E(i, 1) = \log(1/3) \approx 1.1$, which remains for the two following steps (i.e. $h = 2$ and 3). Observe that the additional all-to-all connections between the nodes in the second and third steps have no effect in changing the respective diversity entropy, as they do not affect the respective probabilities $p(i, j, 3)$. The situation depicted in (d) involves self-avoiding random walks with different lengths, namely 1, 2 and 3. Because the moving agent is assumed to remain at its termination node, the diversity entropies do not change along the 3 initial steps. Though this assumption implies eventual degeneracies such as obtaining the same diversity entropy signatures for the structures in (c) and (d), the distinction between such cases can be easily accomplished by considering additional measurements such as the length of the walks. Finally, the situation shown in (e) involves converging connections at steps 1 and 2, which contribute to reducing the diversity of the random walks. Observe that the alternative assumption of removing the moving agent after it has reached a termination node would imply identical diversity entropy signatures for both structures in (d) and (e).

Given a network with N nodes, the maximum diversity entropy obtained at any step is given when $p(i, j, h) = 1/N$, implying

$$W = -1/N \sum_{j=1}^N \log(1/N) = \log(N) \quad (2)$$

Figure 3 shows the maximum diversity entropies for several values of N . Therefore, as all networks considered in this article involves $N \approx 100$, the diversity entropy is maximally bound to $W = \log(1/100) \approx 4.61$.

A particularly interesting situation occurs when each node at each level h leads exclusively to a constant number $\langle k \rangle$ of new nodes in the subsequent level $h + 1$ (see Figure 4). In this case, $p(i, j, h) = 1/\langle k \rangle^h$, so that

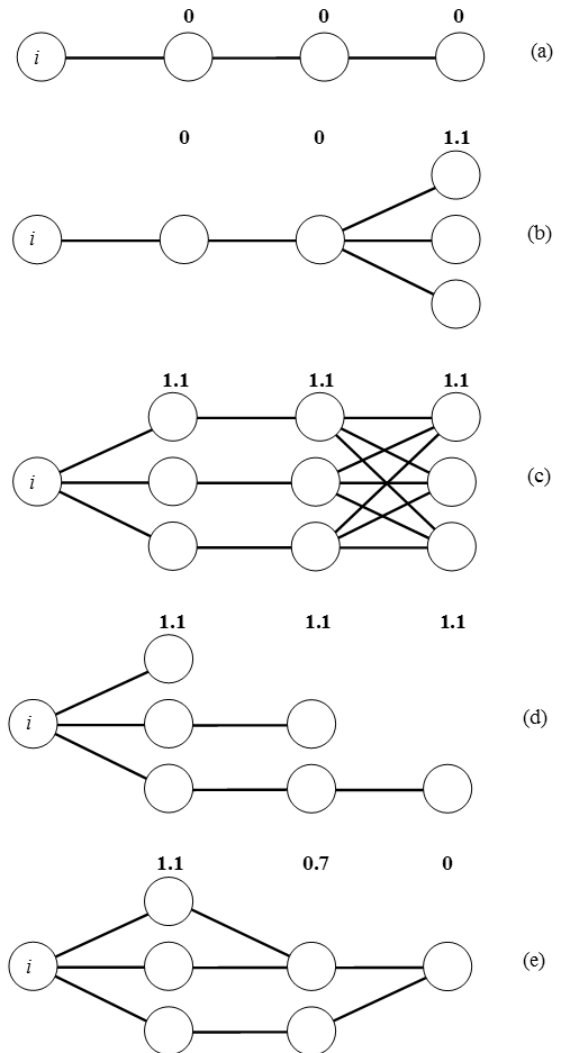


FIG. 2: Illustrations of diversity entropy signatures (the diversity entropies are shown in bold): (a) as the paths from node i are all equal for this case, the entropies are null for all values of h ; (b) the divergence of edges at $h = 3$ implies the increase of the diversity entropy to $1/\log(3) \approx 1.1$ at that level; (c) the presence of all-to-all connections between the nodes at steps 2 and 3 has no effect in increasing the entropies at level $h = 3$; (d) because the moving agent remains at each terminal node after reaching it, the entropy does not change at the successive steps for this case; (e) converging edges (at the second and third steps in this particular example) can lead to decrease of the diversity entropy along h .

$$E(i, h) = - \sum_{j=1}^{\langle k \rangle^h} \log(\langle k \rangle^h / \langle k \rangle^h) = h \log(\langle k \rangle) \quad (3)$$

Therefore, the diversity entropy will tend to increase (or remain null for $\langle k \rangle = 1$) with h at constant rate

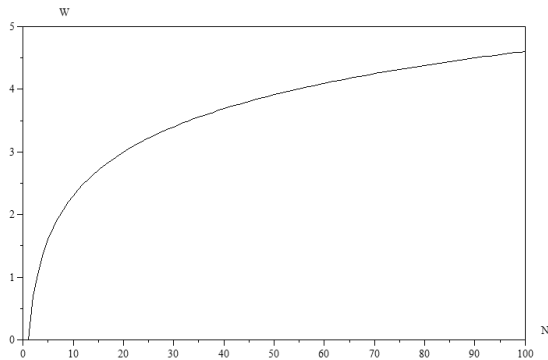


FIG. 3: The maximum diversity entropy which can be obtained for networks with N nodes.

$\log(\langle k \rangle)$. This situation involves an infinite and completely regular network (i.e. each node has the same degree $\langle k + 1 \rangle$). As complex networks are often analyzed with respect to regular or nearly regular counterparts (e.g. ER model), it is useful to consider the above configuration as a reference. For instance, the situation in which the diversity entropy tends to increase almost linearly with h along an interval can be understood as an indication that the network is mostly regular along that interval. However, it should be born in mind that linear increase of the diversity entropy can also be caused by other structural organizations in complex networks (i.e. constant increase of entropy does not necessarily implies network degree regularity, but the latter necessarily implies linear entropy increase).

As the diversity entropy has been defined for each node i at each step h , it provides an individual signature associated to each node (see Figure 1), which can be valuable while investigating dynamics emanating from that node. However, it is often interesting to get an overall idea of the diversity entropy dynamics considering all the nodes in the networks. This can be immediately obtained in terms of the average and standard deviation of the diversity entropy at each step h , i.e.:

$$\langle E(h) \rangle = \frac{1}{N} \sum_{i=1}^N E(i, h) \quad (4)$$

$$Var\{E(h)\} = \frac{1}{N} \sum_{i=1}^N (E(i, h) - \langle E(h) \rangle)^2 \quad (5)$$

$$\sigma_{E(h)} = +\sqrt{Var\{E(h)\}} \quad (6)$$

The algorithm adopted for picking a random path is simple and, given each starting node i , involves performing M self-avoiding random walks along the initial S steps (in this work, $S = 10$). Therefore, for each node $i = 1, 2, \dots, N$, an accumulator array V of dimension

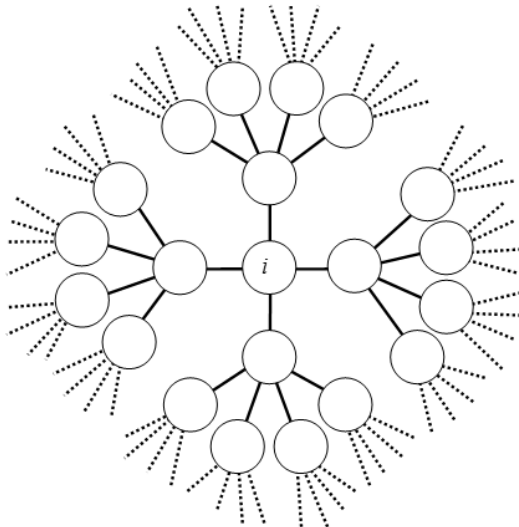


FIG. 4: An example of a situation where the diversity entropy increases linearly with the steps h .

$S \times N$ is kept in order to store the number of visits to each of the network nodes after starting from i . At every step $h = 1, 2, \dots, S$ along each of these M self-avoiding walks, the moving agent is found at a node j and the element $V(h, j)$ of the accumulator vector is incremented by one. After completing the M self-avoiding walks starting from node i , the probability of visits to nodes can be estimated as $p(i, j, h) = V(h, j)/M$. Recall that once the moving agent reaches a termination node, it remains there for all remaining steps. For $N = 100$, the situation considered for all networks in this article, the probabilities have been experimentally found to have converged to less than 5% stability for $M = 200$, which is henceforth adopted.

D. Optimal Dimensionality Reduction by Stochastic Transformations

In several situations, especially for nearly uniform network (i.e. nodes having most nodes with similar properties, such as degree), the diversity neighboring entropies along the steps of the signatures obtained for each node i will tend to be strongly correlated. Indeed, recall that each node i in the network will be mapped into a 10-dimensional feature vector (the diversity entropy signature), which is a relatively high dimensional space, impossible to be visualized. It is possible, and useful, to reduce the dimensionality of such measurement spaces by using optimal stochastic linear transformations such as *principal component analysis* and *canonical projections*

(e.g. [5, 22]).

The former of these approaches allows the measurement space to be optimally projected into $m \leq S$ dimensions, $m \geq 1$, while maximizing the variation of the observations along the first transformed, new variables (e.g. [5, 22]). The transformed variables, which are linear combinations of the original measurements, are guaranteed to be completely *uncorrelated*. The latter transformation (i.e. canonical projections) allow the measurement space to be optimally projected into a smaller dimensional space while maximizing the separation of the categories of observations, in the sense of maximizing the interclass variation and minimizing the intraclass dispersion (e.g. [5, 23]). In both cases, the resulting transformed variables are *linear combinations* of the original measurements.

Though still rarely applied in complex network research, such optimal stochastic transformations can be a real help in organizing and simplifying the analysis and classification of complex networks (e.g. [5]). In this work, the principal component approach is used in order to decorrelate the diversity entropy signatures obtained for each of the nodes in a given complex network, while the canonical projections method is applied in order to obtain visualizations of the distribution of several realizations of 6 different types of complex network models. Additional information about the canonical projections analysis, which is mathematically more sophisticated than the principal component approach, can be found in [5, 23]. The principal component analysis, used to decorrelate the diversity entropies in this work, is described as follows.

Let \vec{f} be the feature vector containing the S measurements obtained for each observation $i = 1, 2, \dots, N$. In the present work, each node i (an observation) is mapped into a diversity entropy signature (the feature vector) of dimension $S \times 1$. The elements $C(i, j)$, $i, j = 1, 2, \dots, S$ of the *covariance matrix* of such a dataset can be estimated as

$$C(i, j) = \frac{1}{N-1} \sum_{p=1}^N (v(i) - \mu_i)(v(j) - \mu_j) \quad (7)$$

where μ_a is the average of $v(a)$, $a = 1, 2, \dots, S$. Observe that $C(i, j) = Var(i)$ whenever $i = j$. Also, we have that the covariance matrix C is necessarily symmetric.

Let γ_i , $i = 1, 2, \dots, S$ be the eigenvalues of the covariance matrix, ordered so that $\gamma_1 \geq \gamma_2 \geq \dots \geq \gamma_S$, and let \vec{q}_i be the respectively associated eigenvectors. The principal component analysis can be obtained by performing the following stochastic linear transformation

$$\vec{g} = \begin{bmatrix} \leftarrow & \vec{q}_1 & \rightarrow \\ \leftarrow & \vec{q}_2 & \rightarrow \\ \dots & \dots & \dots \\ \leftarrow & \vec{q}_m & \rightarrow \end{bmatrix} \vec{f} \quad (8)$$

where $m \leq S$, $m \geq 1$, \vec{f} and \vec{g} have respective dimensions $S \times 1$ and $m \times 1$. Therefore, the new measurements (transformed variables) belong to a space of reduced dimensionality $m \leq S$. The new measurements associated to the largest eigenvalues are called the *main* variables or components. Observe that each of the new measurements is a linear combination of the original measurements, while the eigenvalues γ_i , $i = 1, \dots, m$, correspond to the variances of the new measurements in \vec{g} . So, it is reasonable to include in the transformation matrix only the eigenvectors associated to eigenvalues which are particularly large, in order to encompass the greatest part of the original variation of the observations. Also, observe that the relative weight of each of the original measurements used in the linear combinations defining the new variables can provide an indication about the importance of the respective original measurements. Because the feature vectors considered in this work have all the same nature and potential dynamic range (recall that all the elements of the diversity entropy signature are entropies vary between 0 and $\log(N)$), there is no need for preliminary standardization of the original measurements (e.g. [5]).

III. RESULTS AND DISCUSSION

The diversity entropy methodology has been applied at the level of network categories and individual nodes. In the former case, the overall diversity was characterized with respect to the average and standard deviation of the diversity entropies obtained for each realization of the networks. The latter investigation targets the estimation of the diversity entropy signature at the individual node level, which allows the partitioning of each network into subgraphs of similar diversity. These two types of investigations, at the network and individual node levels, are described in the respective following sections.

A. Network Level

We start our diversity investigation by looking at the averages and standard deviations of the diversity entropy signatures obtained for the realizations of each of the 6 considered network models. More specifically, a total of 50 realizations were performed for each of the six complex network models considering $N = 100$ and two average degrees: (a) $\langle k \rangle = 6$ (i.e. $m = 3$) and (b) $\langle k \rangle = 10$ (i.e. $m = 5$). For each of such realizations, 200 random pathwalks were performed starting from each of the nodes, and the respective entropies $E(i, h)$ were estimated for $h = 1, 2, \dots, 10$. The average $\langle E(h) \rangle$ and standard deviations $\sigma_{E(h)}$ of these diversity entropy values were obtained for each of the 50 network realizations for each of the 6 considered models and are shown in Figures 5 and 5 respectively to $m = 3$ and $m = 5$.

A series of interesting results can be inferred from the

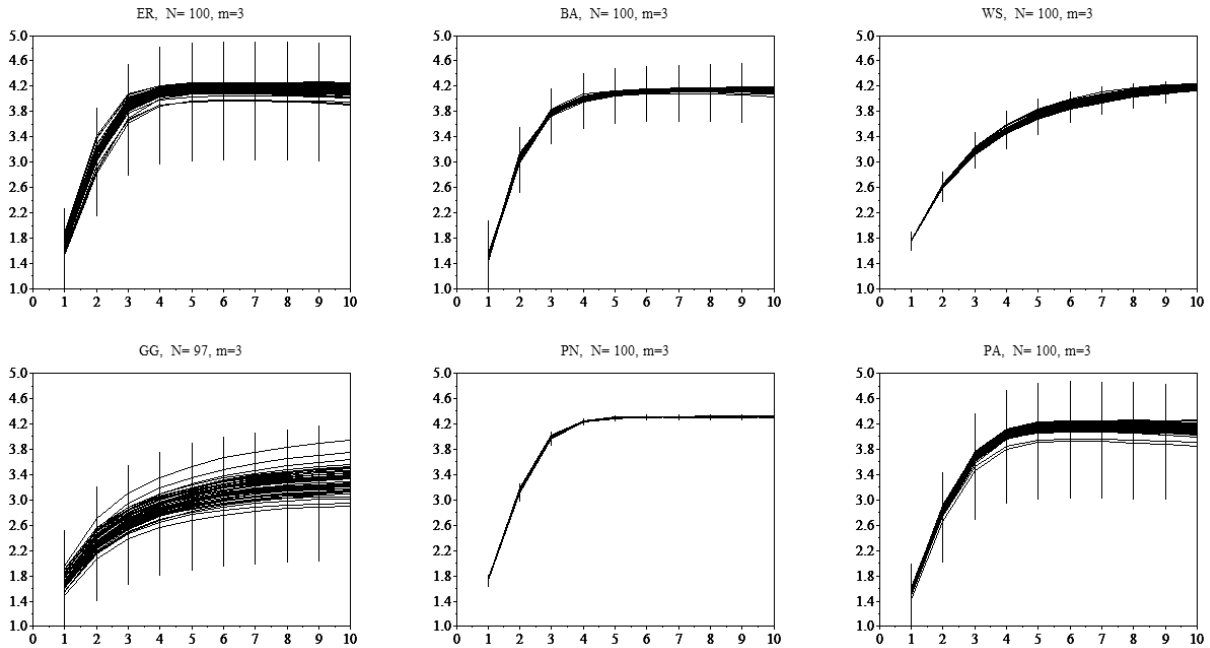


FIG. 5: The average \pm standard deviations of the diversity entropies obtained for each of the networks considered for each of the six complex networks models assuming $N = 100$ and $m = 3$ (i.e. $\langle k \rangle = 6$).

curves in those figures. First, observe that markedly different and distinctive curves and standard deviations were obtained for the networks belonging to each of the considered models. Two general behaviors can be distinguished in both figures: the steeper increase of the diversity entropy with h obtained for the ER, BA, PN and PA modes as opposed to the more gradual increase verified for the WS and GG models. These two types of transient dynamics can be observed for both $m = 3$ and $m = 5$. In the case of the transient evolutions observed for the ER, BA, PN and PA models, the diversity entropy tended to reach stabilization near the maximum expected value for $N = 100$ (i.e. 4.60) after the three or four initial steps. This suggests that the self-avoiding paths in these networks tend to reach almost all nodes after just a few steps. The more gradual increase of entropy observed for the WS and GG models indicates that the moving agent takes substantially more time to cover a smaller portion of the nodes. This is a consequence of the fact that, though nearly regular (i.e. similar degrees for all nodes), these two types of networks are characterized by having pairs of nodes which are either connected through many short paths (adjacent nodes) or virtually unconnected. More informally, given two nodes i and j of a network, the *adjacency* between them can be quantified in terms of the number of short (i.e. up to a maximum length) self-avoiding paths interconnecting those nodes; the higher this number, the more adjacent the pair of nodes is.

Another interesting result regards the maximum entropy values, reached for large values of h . Except for the GG model, all other types of networks tended to entropies around 4.0 in the case of $m = 3$. A similar result can be observed for $m = 5$, though the plateau entropies tended to be higher than those for $m = 3$ in most models. Interestingly, quite similar limiting entropy values have been obtained for BA and PN networks irrespectively of the average degree. By comparing the respective curves in the two figures, it becomes clear that the higher average degree (i.e. $m = 5$, implying $\langle k \rangle = 10$) tended to reduce the standard deviations for *all* models. Though at first surprising, this effect is ultimately a simple consequence of the fact that increasing the average degree of finite networks tends to make them more regular, implying in more self-avoiding paths covering the same set of nodes. Observe that at the extreme situation in which the network is fully connected, all path-walks will involve all nodes, implying null variance of the diversity entropy. The higher average degree also tended to change the shapes of the curves by implying a steeper increase along the initial step, which is also a consequence of the above observed regularizing effect.

Another interesting result which is evident from Figures 5 and 5 are the markedly distinct standard deviations obtained for each model. Confirming previous investigations [18, 19], the PN model presented the more regular features, with almost null standard deviations of the diversity entropies for either $m = 3$ or $m = 5$. Al-

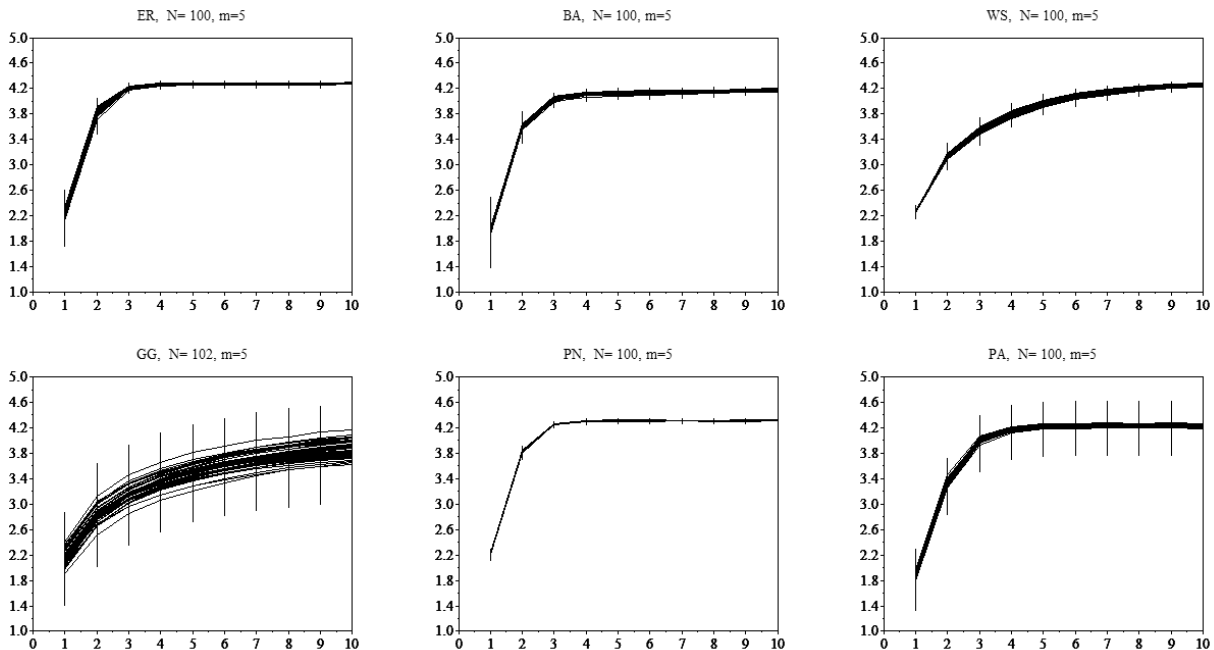


FIG. 6: The average \pm standard deviations of the diversity entropies obtained for each of the networks considered for each of the six complex networks models assuming $N = 100$ and $m = 5$ (i.e. $\langle k \rangle = 10$).

lied with the fast increase of diversity entropy exhibited by this model, the extremely low variance of diversity entropies makes of the PN a choice model for achieving high and uniform diversity signatures. To a great extent, such properties favoring diversity are a consequence of the fact that, unlike the WS and GG models, any pair of nodes in the PN structures tend not to be adjacent in the sense of being interconnected by many short paths. Recall that the ER, WS, GG and PN are all network models characterized by high degree regularity, so that what makes them so different regarding diversity is ultimately the adjacency between pairs of nodes, which is optimally broken in the PN model.

In order to complete our analysis of the diversity entropy signatures for networks belonging to the 6 distinct considered models, we now apply the canonical projection method (see Section IID). We use this method to project the original 10-dimensional entropies space into a 2-dimensional space so as to maximize the separation between the clusters of networks belonging to each category. Figure 7 shows the cluster distributions obtained for $m = 3$ (a) and $m = 5$.

It is clear from Figure 7, where v_1 and v_2 correspond to the two principal canonical variables, that the 6 categories of networks yielded two supergroups: one formed by $\{GG, WS\}$ and the other by $\{ER, BA, PN, PA\}$ (observe the different ranges of values for the two axes). This is in complete agreement with the two main types of diversity dynamics identified for those networks (i.e.

steeper and more gradual increase of the entropies). In addition to confirming that previous result, the canonical projections showed that the ER and PN have marked similarity between their diversities (i.e. the clusters for these two models were mapped nearby in the projected space). The smallest dispersion of the diversities obtained for the PN model are clearly reflect in the dense cluster obtained for that category of networks. Interestingly, the ER and PA clusters tended to change positions considerably for $m = 3$ and $m = 5$.

Additional results can also be obtained by considering the weights of the original measurements in the linear combinations defining the two canonical variables v_1 and v_2 , shown in Table I. We concentrate attention on the absolute values of the weights in Table I. In the case $m = 3$, we have that the two first canonical variables v_1 and v_2 are by the diversity entropies for $h = 1, 2, 4$ and 7 , which are the main measurements responsible for the optimal separation between the 6 models in the case $m = 3$. Observe that 3 out of these 4 variables correspond to entropies at the initial steps (i.e. $h = 1, 2$ and 4). The most important measurements in the composition of the two canonical variables for $m = 5$ are the diversities obtained for $h = 1, 2, 3, 4$, all of which with weights larger than 0.5. Again, the measurements greatly contributing to the separation of the 6 network categories were the initial diversity entropies. The dominant contribution of the initial entropies is completely reasonable because most the diversity signatures tend to become stable and

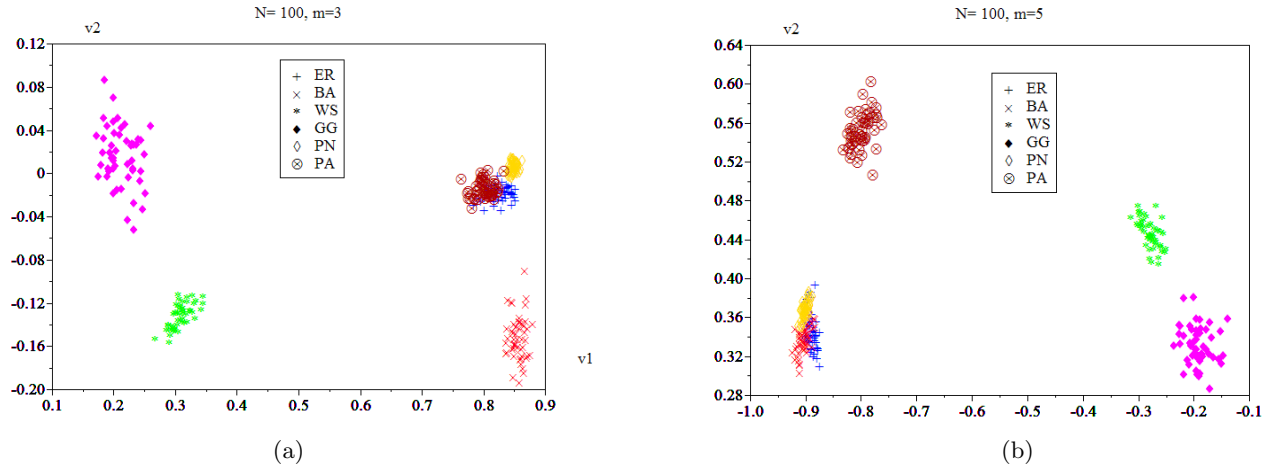


FIG. 7: The clusters of networks, for $m = 3$ (a) and $m = 5$ (b), after being canonically projected from 10 to 2 dimensions so as to maximize the separation between the six categories of networks.

similar after 3 or 4 steps. Such results indicate that, if the main purpose of the analysis is to separate the 6 network types, it is mostly enough to consider the 4 initial entropies in each signature.

$m = 3$		$m = 5$	
$v1$	$v2$	$v1$	$v2$
-0.48	0.52	0.52	0.15
0.02	-0.38	-0.31	-0.61
0.27	-0.03	-0.63	-0.05
0.53	0.56	-0.06	0.57
-0.02	0.30	-0.01	0.09
0.29	-0.08	0.19	0.33
-0.56	-0.30	-0.01	0.17
-0.15	-0.31	0.34	-0.20
0.01	0.02	0.18	-0.30
0.03	-0.06	-0.22	-0.08

TABLE I: The weights of the original measurements assigned by the canonical projections method in order to best separate the 6 categories of complex networks in the 2-dimensional projections for $m = 3$ and $m = 5$.

B. Individual Node Level

Having investigated how the diversity entropies behave in each of the 6 considered network categories, we now turn our attention to the diversity entropy signatures obtained at the level of individual nodes. In order to do so, we selected a network of each type and obtained the respective signatures shown in Figure 8 and 8, with respect to $m = 3$ and $m = 5$. Similar signatures were obtained

for other realizations of each of the 6 types of networks. The geographical network considered in this analysis is shown in Figure 12.

Most of the results and explanations presented in the previous analyses at the network level can be immediately extended to the signatures in these curves. First, the dispersion of the signatures tend to be smaller for $m = 5$ than for $m = 3$. Very similar signatures were obtained for all nodes in the PN network, which confirms the regularity of this model. The two types of transient dynamics, namely steeper for the ER, BA, PN and PA networks and more gradual for the WS and GG structures, were again observed. The most interesting additional information provided by the presentation of the individual node signatures regards the relative dispersion obtained for each case. Observe that particularly distinct diversity signatures were obtained for the GG structure. This is mainly a consequence of the higher structural modularity found in this type of network (see Figure 12).

Additional insights about the measurement structure in each of the networks can be obtained by applying principal component analysis to each of the datasets in Figures 8 and 8 in order to obtain 2-dimensional visualizations of the distribution of the respective diversity signatures. The projection obtained from $m = 3$ is shown in Figure 10 (the projections for $m = 5$ are very similar and are not shown in this article). Recall that each point in these plots corresponds to each of the nodes in the respective network. Quite distinct clusters were obtained for each of the networks. The ER network yielded a 2-dimensional projection which still shows a high degree of correlation between the two PCA variables (corresponding to each of the 2 axes in Figure 10). Interestingly, a group of nodes (namely 56, 34, 51, 90, 28 and 63) resulted separated from the main correlated cluster. The 2-dimensional

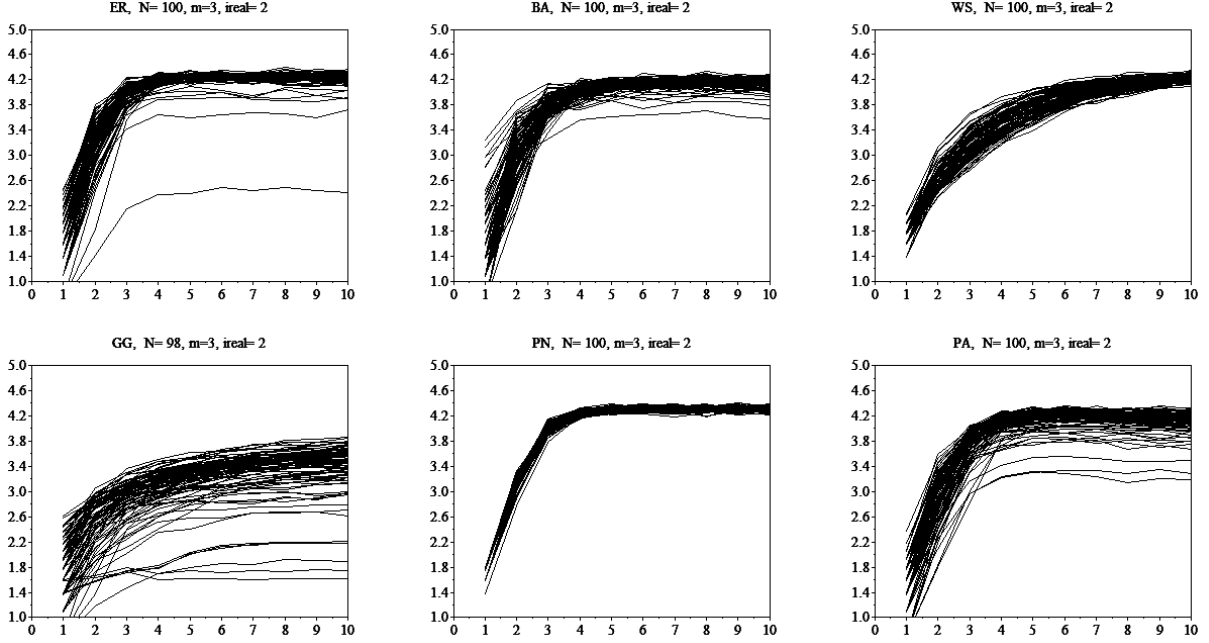


FIG. 8: The average \pm standard deviations of the diversity entropies obtained for each node in a sample of each of the six complex networks models assuming $N = 100$ and $m = 3$ (i.e. $\langle k \rangle = 6$).

PCA projection obtained for the BA network resulted less correlated than that obtained for the ER structure, and also included some outliers. The cluster yielded by the PCA projection of the WS signatures is more compact than those obtained for the ER and BA networks, but still shows some positive correlation between the two principal variables. The distribution obtained for the GG structure presented little correlation between the principal variables and a large dispersion of points. Contrariwise, the projection of the diversity entropy signatures for the PN network yielded the most compact cluster, confirming once again the enhanced regularity of this type of network. Finally, the PA network led to a cluster in the projected space characterized by medium dispersion and slight correlation between the two principal variables.

Additional insights about the influence of the measurements (i.e. the diversity entropies) in the definition of the clusters in Figure 10 can be obtained by considering the respective weights of the original measurements in the linear combinations defining the two main principal variables $pca1$ and $pca2$, which necessarily resulted completely uncorrelated. Observe that the variance of $pca1$ is much wider than that of $pca2$. Such weights are given in Table II. It is clear from the values in this table that, for all cases, the first variable corresponds very closely to the arithmetic average of the diversity entropies for $h = 1$ to 10. Because of its largest variance, this first principal variable is particularly relevant as a single quantification of the individual node diversities. This summarizing

measurement is henceforth called the *overall diversity* of each node. The second principal variable is mainly composed by the initial 3 or 4 diversity entropies, confirming the importance of the initial diversities already identified in the previous section regarding the best separation of the network types.

In order to conclude our investigation of the diversity entropy signatures at the individual node level, we consider the GG network chosen for the above examples (see Figure 12) for a more systematic investigation of the diversities. The choice of this type of network is justified because it is the only case among the considered categories which incorporates the spatial positions of each node and because this type of network tends to exhibit structured modularity (i.e. spatial and topological communities).

Because the first principal variable has been verified to correspond very closely to the arithmetic average of the diversity entropies for all network types, we adopt this value in order to summarize the diversity of each node in the chosen network. Figure 11(a) shows an enlarged version of the PCA projection of the diversity entropies obtained for this geographical network. Because of the right-skewed distribution of the density of the points in this projection, we consider a new projection obtained by taking the exponential of the first PCA variable, henceforth represented as $exp(pca1)$. This new projected distribution is shown in Figure 11(b). A more uniform distribution of points is now obtained. We now subsume

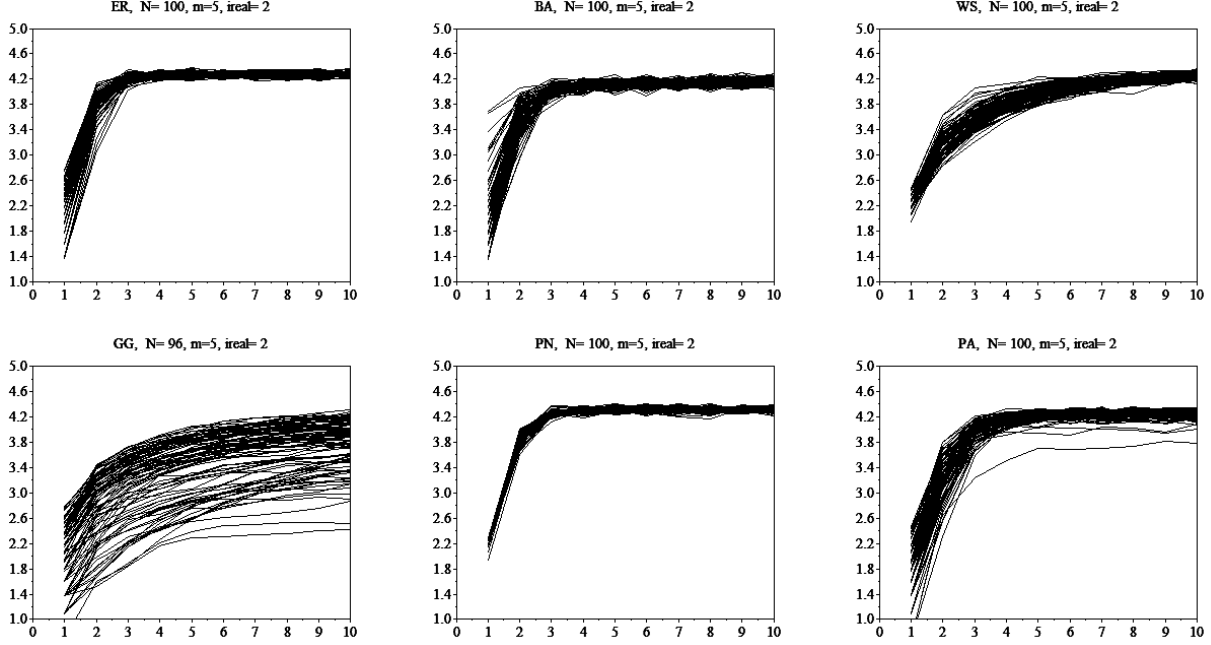


FIG. 9: The average \pm standard deviations of the diversity entropies obtained for each node in a sample of each of the six complex networks models assuming $N = 100$ and $m = 5$ (i.e. $\langle k \rangle = 10$).

ER		BA		WS		GG		PN		PA	
<i>pca1</i>	<i>pca2</i>	<i>pca1</i>	<i>pca2</i>	<i>pca1</i>	<i>pca2</i>	<i>pca1</i>	<i>pca2</i>	<i>pca1</i>	<i>pca2</i>	<i>pca1</i>	<i>pca2</i>
0.14	0.75	0.12	0.91	0.15	-0.04	0.19	0.81	0.14	0.50	0.13	0.67
0.26	0.56	0.25	0.32	0.23	0.47	0.26	0.45	0.25	0.74	0.24	0.60
0.32	0.12	0.32	0.06	0.28	0.54	0.30	0.13	0.32	0.23	0.31	0.25
0.34	-0.08	0.33	-0.04	0.31	0.35	0.32	-0.04	0.34	-0.07	0.34	-0.04
0.34	-0.11	0.34	-0.07	0.33	0.19	0.33	-0.09	0.34	-0.09	0.34	-0.11
0.34	-0.12	0.34	-0.09	0.348	-0.05	0.34	-0.13	0.34	-0.16	0.35	-0.13
0.34	-0.13	0.34	-0.10	0.35	-0.16	0.34	-0.14	0.34	-0.14	0.35	-0.15
0.34	-0.13	0.34	-0.08	0.36	-0.26	0.35	-0.15	0.34	-0.16	0.34	-0.16
0.34	-0.13	0.34	-0.12	0.37	-0.30	0.35	-0.16	0.34	-0.18	0.34	-0.16
0.34	-0.13	0.34	-0.12	0.40	-0.38	0.35	-0.18	0.34	-0.16	0.34	-0.16

TABLE II: The weights of the original measurements assigned by the principal component analysis method in order to completely decorrelate the diversity entropy signatures for each of the networks representing each of the 6 categories of networks.

the new variable $exp(pca1)$ into 9 intervals identified by the colors in Figure 11(b). Observe that, because $pca1$ is very close to the arithmetic average of the diversity entropies for the various values of h , the diversity of the nodes increase from left to right in both Figures 11(a) and (b). Figure 12 shows the original GG structure with its nodes colored according to the overall diversity intervals in Figure 11(b).

A series of interesting results can be identified. First, observe that the nodes belonging to more external structures tended to present the smallest overall diversities (in black). All extremity nodes (i.e. nodes with degree 1)

are characterized by the smallest diversity. At the same time, the more densely connected groups of nodes tended to exhibit higher diversity, with node 40 presenting the largest diversity in this network. Indeed, the dense connectivity of the groups of nodes below and above node 40 allow several self-avoiding random walks to evolve from that node. Though such facts seem to suggest a strong correlation between diversity and node degree (see [8] for an investigation about the correlation between the frequency of visits to nodes and their degree), this is not the case. As is clear from Figure 13, which presents the scatterplot obtained by considering the node degree and

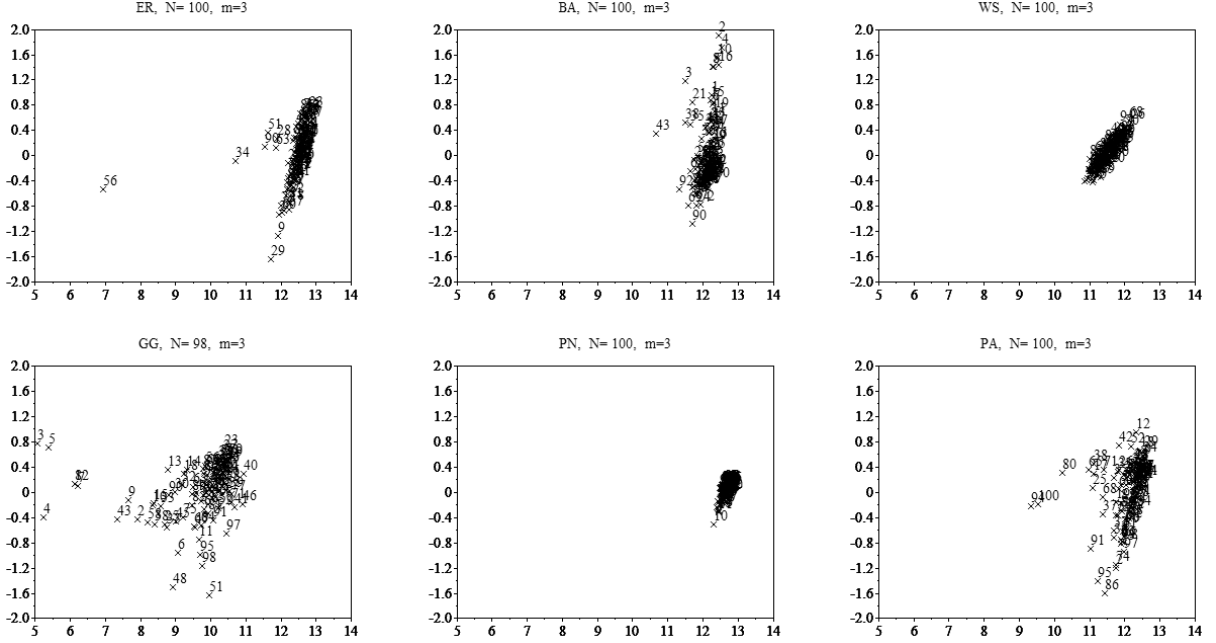


FIG. 10: The two-dimensional projections of the diversity entropy signatures obtained for each of the nodes in a sample of each of the six complex networks models assuming $N = 100$ and $m = 3$ (i.e. $\langle k \rangle = 6$).

overall diversity for the network in Figure 12, these two measurements only a relatively weak positive correlation can be observed between these two measurements. Indeed, several nodes with high degree (i.e. hubs) in the GG structure — including nodes 13, 54, 63 and 73 — do not have high diversity. At the same time, nodes 19, 39, 40 and 79 are hubs characterized by high diversity. Such a weak correlation between node degree and diversity can be accounted by the fact that the degree is an exclusively local property of a node, while the diversity is affected by the topological properties of many other surrounding nodes. As a further illustration of the more intricate nature of diversity, consider the two following very simple networks: (i) a hub whose adjacent nodes are weakly interconnected; and (ii) a hub with strongly interconnected adjacent nodes. In the former situation, after the moving agent leaves the hub to an adjacent node j , it can proceed only to the few nodes connected to j , implying small diversity at $h = 2$ and subsequently. Contrariwise, because of the many interconnections between the nodes adjacent to the hub in situation (ii), many more self-avoiding walks will be possible, increasing the diversity at $h = 2$ and beyond. Therefore, the diversity is also affected by the clustering coefficient around each of the nodes along the self-avoiding walks. Observe also that though most pair of adjacent nodes tend to present similar diversities, this is not necessarily guaranteed (see, for instance, nodes 53 and 54). Another interesting aspect regards the possible relationship between diversity

and community structure. As suggested by the situation of node 46, it could be conjectured that nodes placed between two communities (one above and the other below) would tend to present higher diversity, as the self-avoiding walks emanating from such nodes could proceed relatively freely inside both communities. At the same time, small communities such as that in the lower right-hand corner of the graph in Figure 12 would tend to have nodes exhibiting low diversity. Because diversity is not directly related to betweenness centrality, additional studies are necessary in order to investigate more precisely how diversity and communities are related.

The quantification of the overall diversity of each node allows many interesting practical interpretations and applications. For instance, in case the moving agent is attacking the network, the greatest disruption will be obtained in the cases in which it starts from high diversity nodes, such as 40 and 46. This would be true even if in cases the moving agent destroys the nodes after visiting them. At the same time, distribution of mass of information would be most effectively performed by allocating the sources to nodes with high diversity. Another interesting applications would be to consider the spatial exploration of the network while starting from different nodes. Exploring agents starting from low-diversity nodes will have to invest much more efforts (i.e. steps) in order to explore the network nodes than those starting at higher diversity nodes. Immediate analogies can be drawn with WWW exploration and knowledge acquisition [16], where

each node represents a piece of knowledge which are acquired by the moving agent as it moves through the network. In addition, edge or node failures or attacks taking place at low-diversity regions of the network will have higher changes of causing major disruptions to the connectivity.

It is important to observe that experiments performed considering diversity entropy signatures defined by traditional random walks (i.e. with possibility of repeating edges and nodes) have led to substantially less intuitive and informative results regarding the structure of the analyzed networks.

IV. CONCLUDING REMARKS

Several systems in the real-world involves non-linear transient evolution after starting from well-defined, specific states. Examples of such dynamics are numerous and include WWW navigation, Internet routing, evolution of knowledge and cultural acquisition (e.g. [16]), disease spreading, as well as evolutionary processes leading to new species (phylogenetics), to name but a few. Once the underlying system has been properly represented as a complex network, transient dynamics can be investigated by performing diverse types of random walks. Though several works have been reported involving the traditional random walk, where nodes and edges can be visited more than once, relatively few approaches have concentrated attention in non-linear transient dynamics obtained by performing self-avoiding random walks (e.g. [16, 20, 21]). One particularly interesting aspect of such a kind of transient dynamics concerns its necessarily finite nature (as opposite to traditional random walks) and more purposeful exploration and coverage of the networks, in the sense of connecting nodes with the smallest number of edges. Therefore, the characterization of such a type of dynamics can provide valuable resources not only for understanding the structure of networks, but also for quantifying important dynamics properties such as node coverage and redundancy/resilience.

The current work focused attention on the issue of how diverse are the self-avoiding random walks performed in different types of networks after starting from different nodes. Because we wanted to obtain information about the diversity along the several steps while moving from a specific starting node, a simple sampling algorithm was used in order to estimate the probabilities of visits to nodes required for the diversity entropy calculation. In such a way, diversity entropy signatures can be estimated for every node in different types of networks. The main contributions of the current article are listed and briefly discussed in the following:

Definition of the diversity entropy signature:

An objective way to quantify the diversity of self-avoiding random walks has been described which takes into account the diversity along several subsequent steps along the walk, after starting from an individual node i . Such

an approach allows the discrimination, for instance, between walks which are diverse only at the initial steps and walks which are diverse only at the later steps. The estimation of the diversity in terms of the entropy of the probabilities of visits to nodes provides a natural and intuitive choice for measuring the diversity. A simple but effective sampling algorithm has been suggested which can estimate the probability of visits to nodes at each step along the self-avoiding walks. The diversity entropy signature can be used for several purposes, including the study of network categories and the properties of nodes in specific networks. Both these possibilities have been explored in this article. Though potentially affected by several other topological measurements (e.g. node degree, clustering coefficient and betweenness centrality), the diversity is not necessarily correlated to any of these features, therefore providing complementary information about the topology and dynamics of complex networks.

Characterization of the diversity of several types of networks: The diversity entropy signature has been used in order to investigate the general diversity of categories of networks. In this work, we considered 6 diverse and representative theoretical models: Erdős-Rényi (ER), Barabási-Albert (BA), Watts-Strogatz (WS) and a geographical model (GG) — as well as two recently introduced knitted types of complex networks [18] — the path-transformed BA model (PA) and path-regular networks (PN). The diversity entropy signatures were estimated for all nodes in each realization of each of these models, and summarized in terms of their average and standard deviation for each network. A series of interesting results were obtained, including the verification of the increase of diversity with the average node degree, the existence of two types of transient dynamics (steep and gradual increase along the steps), the high dispersion of diversity observed for the WS and GG models, as well as the surprising uniformity of the diversity signatures for the PN networks. The latter model provides one of the most effective structure ensuring steep increase of diversity for all nodes and can be used in the design of several practical systems such as information dissemination/exploration and transportation systems.

Definition of Adjacency as a principal cause of diversity: The two types of signature regimes identified among the 6 considered theoretical models are at least partially accounted by the degree of adjacency between any pairs of nodes in each network. While the standard adjacency between two nodes simply states that there is at least one edge connecting them, the concept of *degree of adjacency* has been considered in this work in order to take into account the adjacency implemented through longer connections. More specifically, the degree of adjacency between any two nodes in a network at a given path-length is understood as the number of paths of that length connecting the two nodes. By using such a concept, it becomes possible to discriminate between otherwise degree regular models such as ER, WS, GG, PN and PA. More specifically, because of spatial constraints,

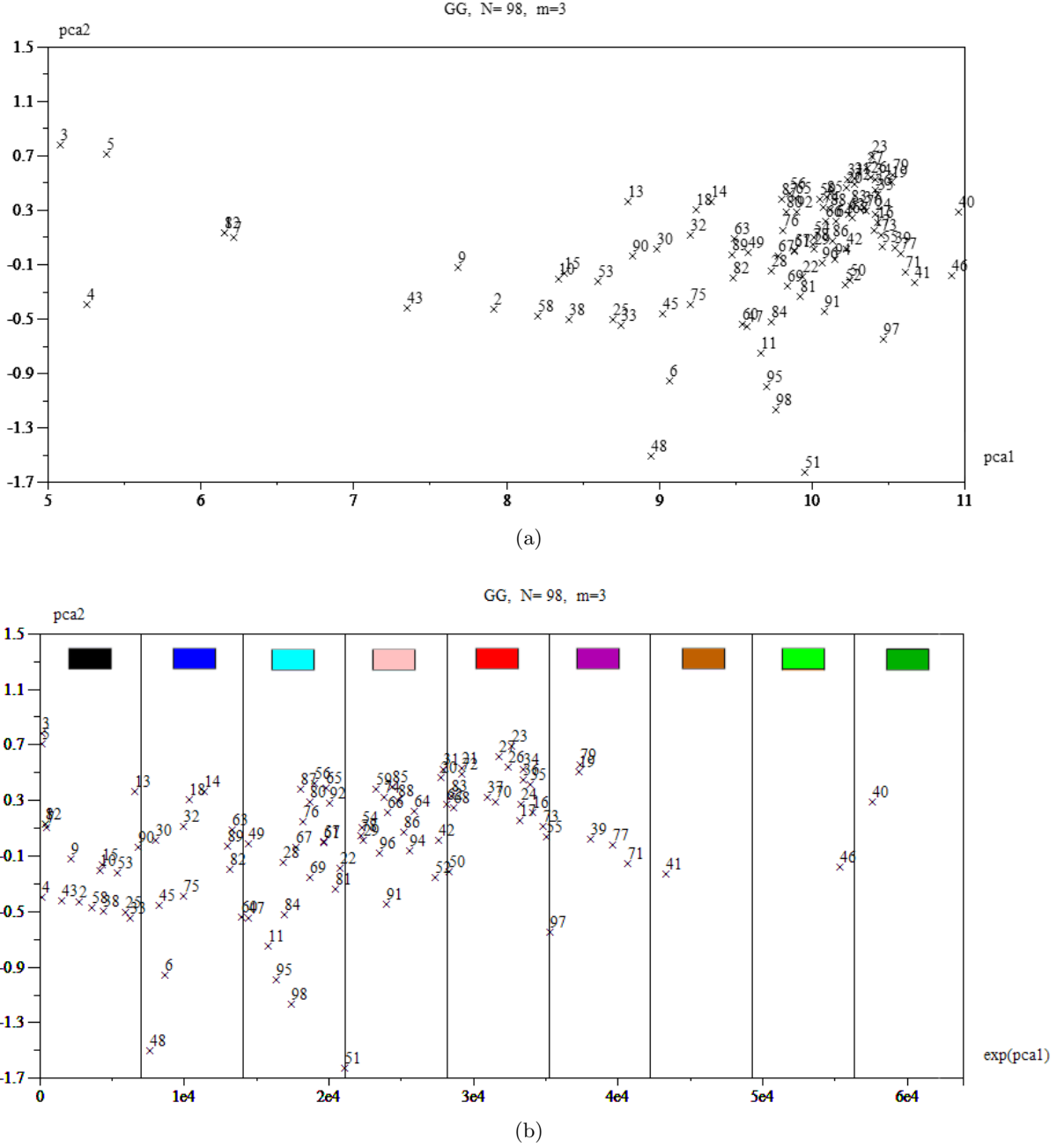


FIG. 11: The PCA projection obtained for the chosen GG network (a), and its transformation (b) obtained by taking the exponential of the first PCA variable, i.e. $exp(pca1)$. The colors identify each of the intervals of the $exp(pca1)$ range.

both the WS and GG structures have most pairs of nodes exhibiting higher degree of adjacency for several path-lengths. Such a local connectivity enhances the chances of termination of the self-avoiding walks, therefore reducing considerably the diversity entropies. Such an effect has been clearly identified in the obtained results, leading to the identification of two regimes of transient evolution of the diversity.

Use of sound multivariate statistics to decorrelated the entropies: Because the diversity entropies at subsequent steps tend to be highly correlated, especially for more regular networks, it becomes essential to extract the most representative information from the signatures by decorrelating the entropies at each step. In this work we have applied two sound and established optimal methods for dimensionality reduction for obtain-

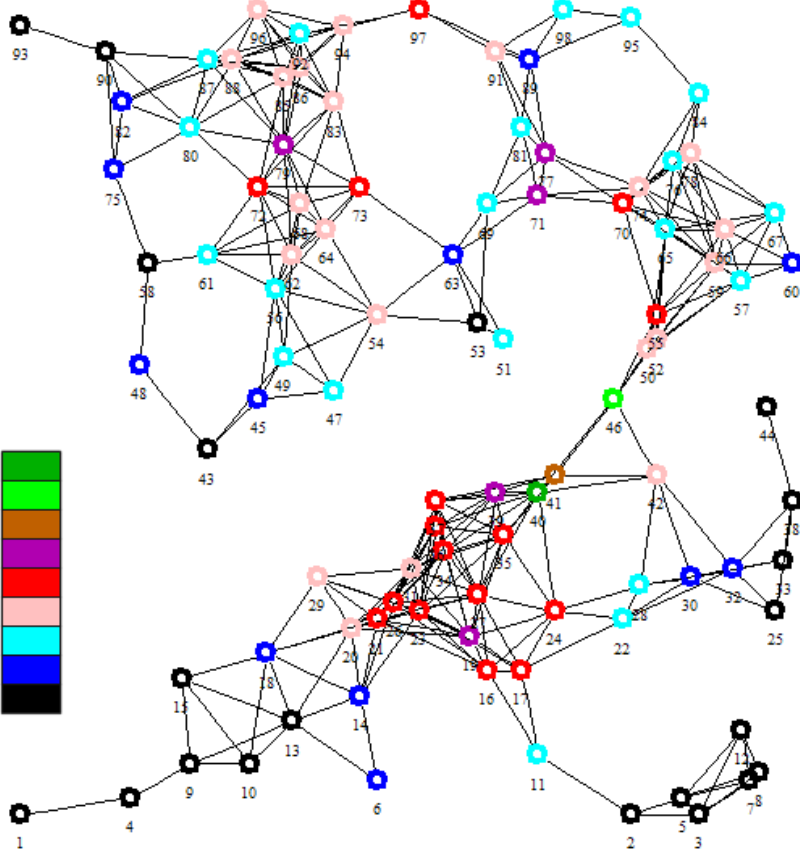


FIG. 12: The GG network with $n = 98$ and $m = 3$ and its nodes colored according to the intervals defined for the exponential of the first pca variable in Figure 11.

ing more representative projections of the diversity signatures. The *canonical projection* methodology, which performs dimensionality reduction in order to optimally maximize the separation between the clusters produced by each category of networks, was applied in this work in order to emphasize the relationship between the diversity structure of the 6 considered models. The weights assigned to each original measurement by this transformation confirmed the special information of the initial 3 or 4 diversity entropies for the discrimination between the considered models. The *principal component analysis* approach was applied in order to decorrelate the entropy signatures obtained for individual nodes in specific networks. In all cases, the first principal variable was found to correspond very closely to the arithmetic average of all entropies. This variable has been used to summarize the diversity of individual nodes of specific networks into a single measurement, called *overall diversity*. Observe that the use of the arithmetic average as a single descriptor has not been imposed a priori, but established as a consequence of optimal decorrelation between the several

diversity entropies. The second principal variable was found to be more strongly affected by the first diversity entropies, confirming the importance of these features.

Characterization of the diversity of several types of networks at the individual node level:

The diversity entropy signature was also investigated at the level of individual node for an example network from each of the 6 considered types of structures. Such an analysis led to results similar to those obtained for the global analysis. By using the principal variable as a single quantification of the diversity of the individual nodes, we were able to study in more detail a sample of GG network, which provides the spatial position of the nodes and exhibit community structure. The overall diversity was estimated for each node and 9 intervals of diversity were defined by binning the exponential values of the overall diversity, which allowed a more uniform distribution of the measurements. The nodes of the network were then identified (colored) according to such intervals, leading to an interesting partitioning of the network in terms of the respective diversities. A series of interesting results

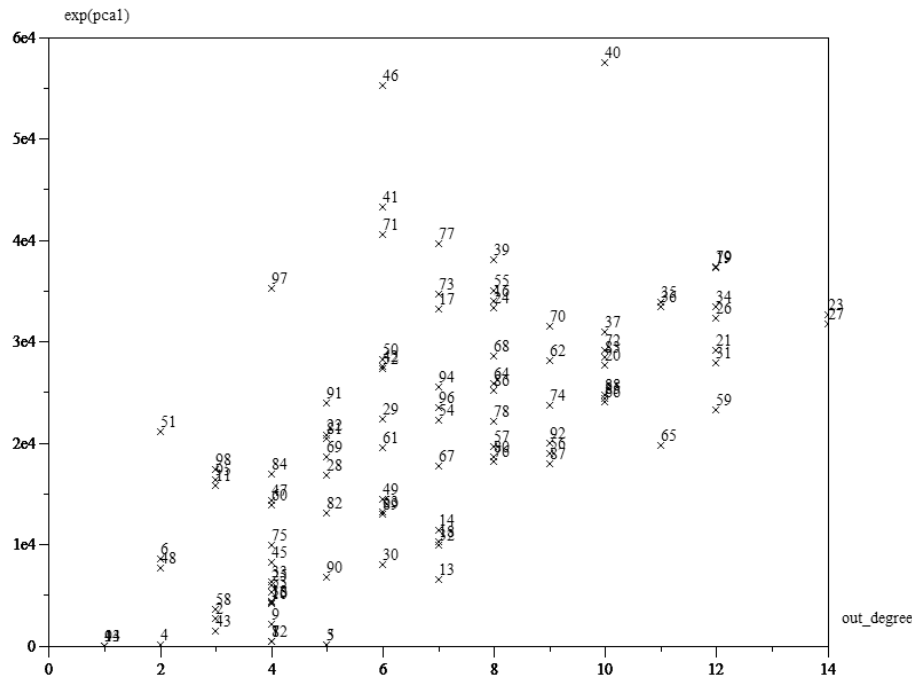


FIG. 13: The scatterplot obtained by considering the overall diversities of the nodes in the GG structure and their respective degrees. Only a weak correlation can be identified between these two measurements.

were obtained. First, the low-diversity nodes tended to appear at the borders of the network, often involving an extremity node. Interestingly, the own concept of diversity can be used to define the network border nodes as corresponding to those which have little access to the remaining network. Second, the more densely interconnected nodes tended to present high diversity. However, no strong correlation has been identified, at least for the considered GG network, between node degree and diversity. Possible relationships between diversity and community structure have also been identified.

Such diverse results are not interesting by themselves regarding several aspects of complex network research, but also open several possibilities for future exploration, including but not being limited to: (i) study of other types of walks, such as preferential; (ii) applications to the characterization of real-world networks; (iii) study of scaling effects, especially with N ; (iv) consider the length of the self-avoiding walks as complementary information

about the structure of the networks; (v) investigate more systematically the relationship between the degree of adjacency and the diversity, especially the possibility if the latter can be predicted by the former; (vi) devise network growth algorithms based on diversity constraints; (vii) use of the diversity to identify particularly weak and stronger points in networks (e.g. with respect to resilience or distribution) and try to enhance such situations; and (viii) investigate further the possible relationship between diversity and communities, especially regarding possible influences between diversity and betweenness centrality.

Acknowledgments

Luciano da F. Costa thanks CNPq (308231/03-1) and FAPESP (05/00587-5) for sponsorship.

-
- [1] R. Albert and A. L. Barabási, *Rev. Mod. Phys.* **74**, 47 (2002).
 [2] S. N. Dorogovtsev and J. F. F. Mendes, *Advs. in Phys.* **51**, 1079 (2002).
 [3] M. E. J. Newman, *SIAM Rev.* **45**, 167 (2003).
 [4] S. Boccaletti, V. Latora, Y. Moreno, M. Chavez, and

- D. Hwang, *Phys. Rep.* **424**, 175 (2006).
 [5] L. da F. Costa, F. A. Rodrigues, G. Travieso, and P. R. V. Boas, *Advs. in Phys.* **56**, 167 (2007).
 [6] P. G. Doyle and J. L. Snell, *Random Walks and electric networks* (Carus Mathematical Monographs, 1984).
 [7] J. P. Sethna, *Entropy, order parameters, and complexity*

- (Oxford University Press, 2006).
- [8] L. da F. Costa, O. Sporns, L. Antiqueira, M. G. V. Nunes, and O. N. Oliveira, *Appl. Phys. Letts.* **91**, 054107 (2007).
 - [9] J. D. Noh and H. Rieger, *Phys. Rev. Letts.* **92**, 118701 (2004), arXiv:cond-mat/0307719.
 - [10] N. Masuda and N. Konno, *Phys. Rev. E* **69**, 066113 (2004), arXiv:cond-mat/0401255.
 - [11] P. Pons and M. Latapy (2005), arXiv:physics/0512106.
 - [12] Z. Eisler and J. Kertesz, *Phys. Rev. E* **71**, 057104 (2005), arXiv:physics/0512106.
 - [13] H. Zhou, *Phys. Rev. E* **67**, 061901 (2003), arXiv:physics/0302032.
 - [14] O. Kinouchi, A. S. Martinez, G. F. Lima, G. M. Lourenco, and S. Risau-Gusman, *Physica A* **315**, 665 (2002).
 - [15] S. J. Yang, *Phys. Rev. E* **71**, 016107 (2005).
 - [16] L. da F. Costa, *Phys. Rev. E* **74**, 026103 (2006).
 - [17] L. da F. Costa (2007), arXiv:0711.1271.
 - [18] L. da F. Costa (2007), arXiv:0711.2736.
 - [19] L. da F. Costa (2007), arXiv:0712.0415.
 - [20] C. P. Herrero and M. Saboya, *Phys. Rev. E* **71**, 016103 (2005).
 - [21] C. P. Herrero, *Phys. Rev. E* **68**, 026106 (2003).
 - [22] L. da F. Costa and R. M. Cesar, *Shape Analysis and Classification: Theory and Practice* (CRC Press, 2001).
 - [23] G. J. McLachlan, *Discriminant Analysis and Statistical Pattern Recognition* (John Wiley and Sons, 1998).
 - [24] Two undirected edges (i, j) and (p, q) are adjacent iff $i = p$ or $i = q$ or $j = p$ or $j = q$.
 - [25] It is sometimes interesting [18, 19] to proceed in two directions, i.e. through two outgoing edges from the starting node. Though interesting, this type of self-avoiding walk is not considered in this work.